Thermal diffusivity of polymers by the flash method

F. C. Chen, Y. M. Poon and C. L. Choy
Department of Physics, The Chinese University of Hong Kong, Hong Kong
(Received 27 September 1976)

We have adopted the flash method to the measurement of thermal diffusivity α of polymers in the temperature range 100–400K. The pulsed radiant energy from a flash tube is applied to the 'front' side of a suspended sample disc, and α is deduced from the exponential decay time constant of the subsequent transient temperature difference between the 'front' and the 'back' side, while correction against radiation loss is made by measuring the much longer decay time of the back-side temperature. Calibration runs on polycarbonate (PC) samples of several thicknesses show that the method is quick, precise and fairly accurate, and the results obtained are in reasonable agreement with previous determinations. We have also carried out measurements on polyoxymethylene (POM), poly(vinylidene fluoride) (PVF_2) and poly(ethylene terephthalate) (PET) and computed their thermal conductivities. Results on POM and PVF_2, which are semicrystalline, are analysed in the framework of several two-phase models, and the effect of crystallization (produced by annealing) on the glass transition behaviour of PET has also been studied.

INTRODUCTION

The flash method for determining thermal diffusivity, α (mainly that of highly radioactive nuclear fuel elements) was first developed by Parker *et al.*[1] in 1961, and has found application to the measurement of α for a number of other solids since[2–6]. The method consists mainly of flashing a short (typically msec) pulse of radiant energy on a sample of carefully chosen geometry, recording the behaviour of the transient temperature at one or more points in the sample, and then deducing α from the curves of the time dependence of the temperature. Like other non-steady-state methods, it has the advantage of being relatively quick and less affected by errors arising from radiation loss or temperature drifts: it is therefore particularly suitable for measuring poor thermal conductors and for high-temperature measurements in general. Furthermore, the use of a flash (usually produced by a laser or a flash lamp) for thermal input allows the use of relatively small sample size and keeps the need for physical contact with the sample to a minimum, thus greatly simplifying the problem of correcting for systematic errors. We have therefore felt that this method is a good alternative to the steady-state method for application to polymers at, say, above the liquid nitrogen temperature, especially in view of the fact that extensive measurements have already been made on their heat capacities, which, together with the diffusivity, would give the thermal conductivity.

In the next section we make use of the formula derived by Cape and Lehman[7] to determine the necessary correction against radiation loss for data obtained in a flash experiment, and also discuss the optimum sample configuration as well as other possible systematic errors.

In the Experimental section we describe an experimental set-up which has been developed for polymer measurements between 100 and 400K: it consists essentially of a commercial photographic flash-light being flashed on a suspended disc-shape sample, the temperature of its front and back surfaces being sensed by attached thermocouple junctions and traced as functions of time on a potentiometric recorder. Estimates of the various errors involved show that one could expect at least the same sort of precision and accuracy, i.e. 3–10%, as similar measurements utilizing other techniques.

We have made measurements on four polymer samples in the above set-up: polycarbonate (PC), polyoxymethylene (POM), poly(vinylidene fluoride) (PVF_2) and poly(ethylene terephthalate) (PET). Details of this work and the results obtained are discussed later.

THEORY OF MEASUREMENT

Cape and Lehman[7] took linearized radiation loss into account and derived the following expression* for the rise in temperature θ_B above the ambient temperature T_0 at the back-side of a cylindrical shaped sample of thermal diffusivity α, density ρ, heat capacity C, emissivity e, radius R and thickness L at time t after a short flash has been applied to the front-side of the sample:

$$\theta_B(r, t) = f(r) \sum_{m=0}^{\infty} (-1)^m A_m \exp(-\omega_m t/t_c) \qquad (1)$$

where r is the radial distance from the symmetry axis of the sample and $f(r)$ is a radial distribution function incorporating the strength of the flash, but it does not concern us here. The other quantities are:

$$\omega_m = \frac{1}{\pi^2}\left[x_m^2 + \left(\frac{L}{R}\right)^2 z^2\right] \qquad (2)$$

$$t_c = \frac{L^2}{\pi^2 \alpha} \qquad (3)$$

* We have made slight changes in notation for convenience.

$$A_m = \frac{2}{\rho CL} \frac{x_m^2}{x_m^2 + 2y + y^2} \tag{4}$$

$$y = \frac{4\sigma e L T_0^3}{\rho C \alpha} \tag{5}$$

σ being the Stefan–Boltzmann constant; z is the first (or smallest) root of the equation:

$$zJ_1(z) = \frac{R}{L} yJ_0(z) \tag{6}$$

where J_n is the Bessel function of nth order. x_m is the mth root ($m = 0, 1, 2, \ldots$) of the equation:

$$\tan x_m = \frac{2yx_m}{x_m^2 - y^2} \tag{7}$$

Equation (1) is valid under the assumption that the flash duration t_f satisfies $t_f \ll t_c$, and that $(R/L)y \leqslant 1$, the latter condition being necessary for neglecting other terms arising from higher roots to equation (6).

To deduce diffusivity α from $\theta_B(r, t)$ the common practice is to neglect radiation effect (i.e. $y = 0, z = 0, x_m = m\pi$) at first and assume a simple exponential rise of θ_B to its final value θ_f, thus deducing α from the half-time $t_{1/2}$ for θ_B to rise from 0 to $\frac{1}{2}\theta_f$. An estimate of the emissivity e would lead to a value for y, from which the radiation effect can be roughly accounted for by the use of a correction curve[7] deduced from equations (1)–(6) in the $y \lesssim 1$ and $(R/L)y \lesssim 1$ limit. However, a different procedure is adopted in our experiment, and the radiation effect is eliminated by a separate experimental determination and through a correction curve valid for relatively larger y. This is carried out as follows.

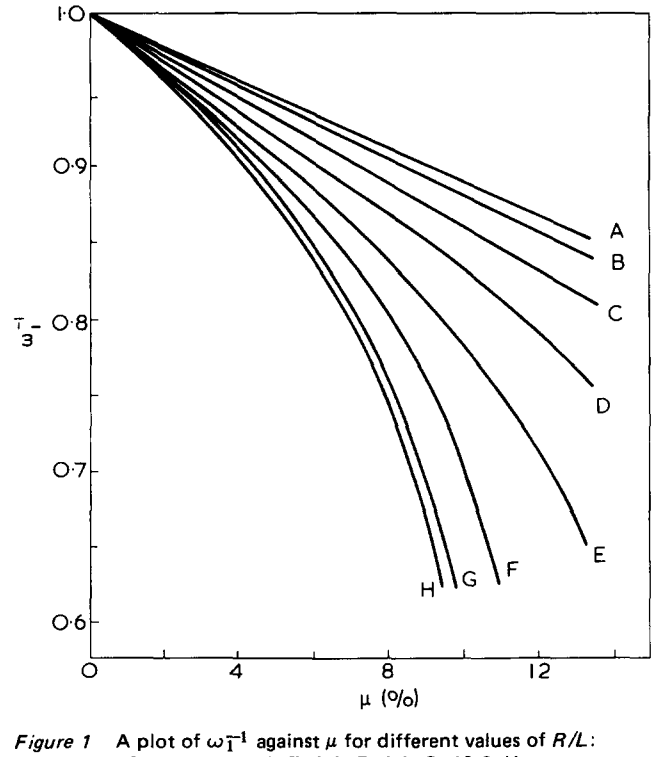

Figure 1 A plot of ω_1^{-1} against μ for different values of R/L: A, 0.1; B, 0.2; C, 0.5; D, 1.0; E, 2.0; F, 4.0; G, 10.0; H, ∞

First we note that the temperature rise θ_F for the front-side of the sample can be shown to be given also by equation (1) provided the $(-1)^m$ factor on the right is left out. The difference $\theta = \theta_F - \theta_B$ is therefore:

$$\theta = 2f(r) \sum_{m \text{ odd}} A_m \exp(-\omega_m t/t_c) \tag{8}$$

Since A_m has a very weak dependence on m and $\omega_m \sim m^2$, only the very first term would contribute for $t \gtrsim 0.6\, t_c$, the $m = 3$ term being less than 1% of it. It is therefore possible to determine the 'front–back' time constant $\tau_1 = t_c/\omega_1$ by a logarithmic plot of θ against t. α can then be computed from τ_1 through equation (3)

$$\alpha = \frac{1}{\omega_1} \frac{L^2}{\pi^2 \tau_1} \tag{9}$$

if the correction factor ω_1^{-1} (~1) is known. It can best be found by first determining the radiation time constant $\tau_0 = t_0/\omega_0$ from the logarithmic decay of θ_B at $t \gg t_c$, thus yielding the ratio $\mu = \tau_1/\tau_0 = \omega_0/\omega_1$. From equation (2) we have:

$$\mu = \frac{x_0^2 + \left(\frac{L}{R} z\right)^2}{x_1^2 + \left(\frac{L}{R} z\right)^2} \tag{10}$$

which, through equations (6) and (7), is an implicit function of y and L/R, and hence, through equation (2), also a function of ω_1 and L/R. In other words, from the measured value of μ and L/R we can deduce ω_1^{-1}, the relation among them being shown in *Figure 1*.

This procedure allows us to determine and correct for the radiation effect unambiguously. It is also more speedy and accurate, since the thermocouple e.m.f. signal given by $\theta_F - \theta_B$ is less affected by electrical and thermal interference or drift than that of θ_B.

EXPERIMENTAL

Sample chamber

As shown in *Figure 2*, the polymer sample (J) in the form of a circular disc of 13 mm diameter and 3 to 6 mm thickness is suspended by three 0.1 mm thick nylon threads from lock nuts on a mounting plate (K), which in turn is fixed between two copper isothermal cylinders (the sample chamber F) suspended at the end of an evacuable thin walled stainless-steel centre tube (A) leading through the liquid nitrogen trap (B) and secured to the top plate. A heat shield (E) attached to the liquid nitrogen trap surrounds the sample chamber and supports the light-guide (G) made of highly polished stainless steel sheet, which by reflection concentrates the radiant energy coming through a plate glass front window (M) from the flash lamp (I) on the outside of the vacuum chamber onto the front surface of the sample. An adjustable and close-fitting light shield (L) mounted on the sample plate (K) prevents the curved and back sides of the sample from direct heating by the flash, and a second glass window thermally anchored to it largely absorbs the room-temperature black-body radiation

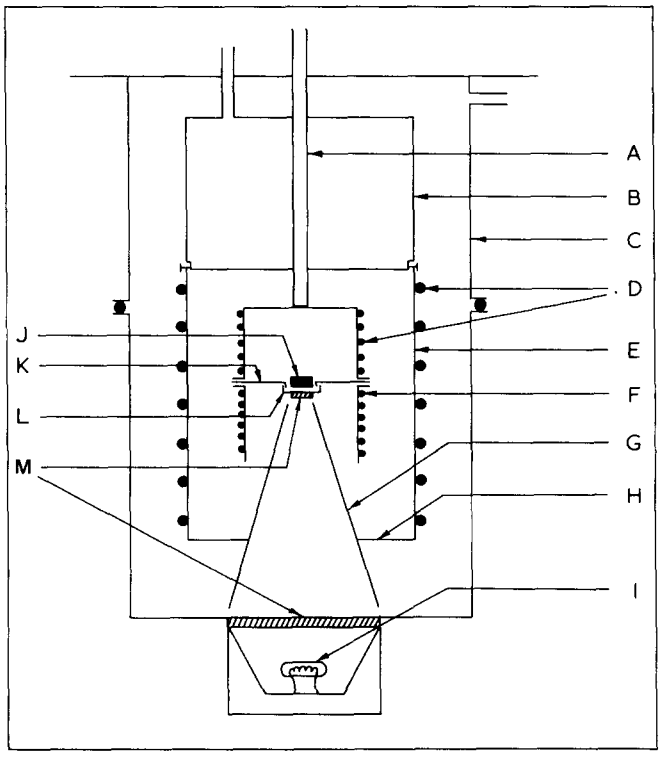

Figure 2 Schematic diagram of the apparatus for thermal diffusivity measurement. A, Evacuable centre tube; B, liquid nitrogen trap; C, vacuum chamber; D, heating wire; E, heat shield; F, sample chamber; G, light guide; H, light guide mount; I, flash lamp; J, sample; K, sample plate; L, light shield; M, glass windows

coming through the light-guide which would otherwise raise the equilibrium temperature of the sample considerably above that of the sample chamber in low temperature runs and also cause a large static temperature gradient in the sample. We found it necessary to use a black lacquer coating on the outside surface of the sample, so as to increase surface absorption and prevent any radiant energy from reaching the interior of the sample.

Two fine-gauge (0.1 mm diameter) copper–constantan thermocouples are attached to the centres of the front and back surfaces of the sample, respectively. The length of the thermocouple wire is about 15 cm so that heat transfer by conduction is negligible. Fine grooves less than 0.1 mm deep are cut on the surface to accommodate the nylon threads and thermocouples, and a very small amount of epoxy (Araldite) is used as the cementing agent. For a typical sample the black coating, the epoxy and the grooves each represent a mass change of about 0.5%, and their combined effect on the results of measurement will be discussed below.

Temperature control and measurements

The liquid nitrogen trap is filled for low temperature (100–300K) runs but otherwise left empty, and high vacuum ($\sim 2 \times 10^{-6}$ Torr) is maintained throughout a measurement except during the initial cool-down period, when some nitrogen gas is let in to speed up the cooling process, which takes 3 to 6 h. The temperature of the sample chamber is sensed by a thermocouple and controlled through electrical heating by an automatic temperature controller (Artronix 5309) against a set-point derived from a microvolt source (Keithley 260). The heat shield can be heated separately with manual power setting. Sample temperature at equilibrium is determined by measuring the 'back' thermocouple output against an ice-point reference cell (Omega TRC Ice-Chamber) on a Leeds and Northrop K-3 potentiometer, with a microvoltmeter (Keithley 150B) as the null detector. For diffusivity measurements transient temperature of either the back (referenced to 0°C) or the front–back difference is first amplified by either the Keithley microvoltmeter (which has better stability but a slower response time of about 0.3 sec) or an a.c. amplifier with adjustable bandwidth (Princeton Applied Research 113), and then traced as a function of time on a 25 x 40 cm *XY* recorder (Hewlett Packard 7005B) with an external time-base.

The flash-lamp which serves as the pulsed radiant heat source is a commercial product for professional photographers (Mecablitz 402 by Metz) but with slight modifications. It delivers sufficient radiant energy to heat up a typical sample by about 1K, and the pulse lasts for about 1 msec, which is more than sufficient to satisfy the short-pulse approximation. The lamp can be flashed either manually or by an automatic control, which in sequence starts the *XY*-recorder time sweep, triggers the flash and switches (by relay) the amplified signal output to the *y*-axis input of the recorder: in case when the 'front–back' temperature difference is observed this mechanism enables us to disconnect the very large but not useful initial output signal from the recorder input. The largest front–back signal recorded for use in data analysis is about 100 μV which corresponds to a temperature difference of 2–3 degrees.

Experimental error

The primary data (τ_1 and τ_0) of our measurements are derived from the ink-recorded traces of electronically amplified thermocouple e.m.f. and as such could have an intrinsic precision of better than 1%. Under experimental conditions we have found that the front–back time constant τ_1 can actually be reproduced to within 2% between different runs if care is taken to avoid electrostatic interference and fluctuations in sample chamber temperature. However, the radiation time constant τ_0 would have a dispersion of 10–15% even under the utmost precautions, the reason being that τ_0 is derived from a smaller signal which has to be measured over a much longer period and is affected more directly by drifts in the sample chamber temperature. Fortunately τ_0 contributes to the final result α only through the correction factor ω_1^{-1}, which has an effect usually less than 10%. Thus the diffusivity data would have an overall precision of about 3%, as could be seen from the various graphs wherein they are plotted.

In addition, we also expect a number of systematic errors. These include the slight static temperature gradient in the sample prior to a flash, non-uniformity in the temperature of the sample chamber, the incoming radiant energy being a pulse with finite duration and having intensity fluctuations over the front surface of the sample, etc. However, the combined effect of the various attachments (nylon threads and thermocouples), adhesives (black coating and epoxy) and grooves on the sample as well as the uncertainty associated with the position of the thermocouple junction is likely to be the most prominent. To see this 'bond' effect more clearly we have made measurements on three PC samples of different thickness (1.50, 2.44 and 3.84 mm) and plotted $(t_c)^{1/2}$ against thickness L for a number of temperatures (*Figure 3*). According to equation (3) ideally these should all be straight lines passing through

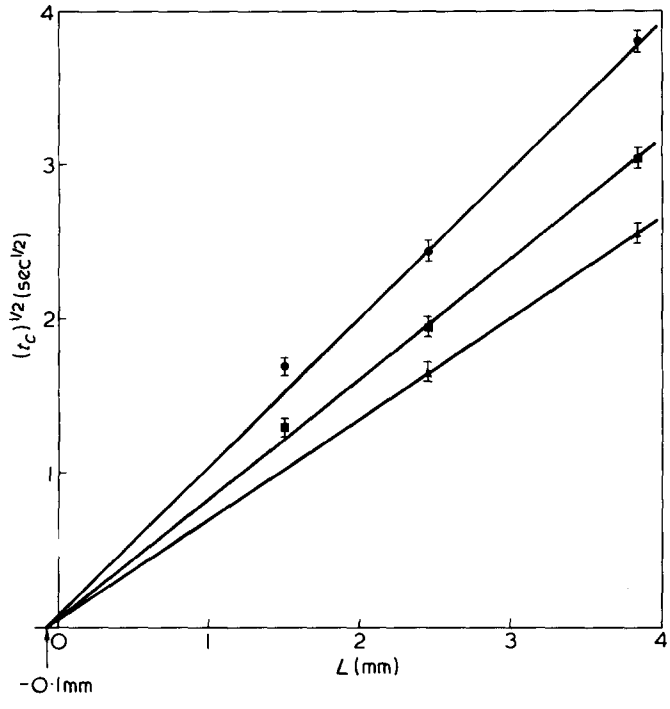

Figure 3 A plot of $(t_c)^{1/2}$ against thickness L of polycarbonate samples at various temperatures: ●, 370K; ■, 210K; ▲, 110K. The ±3% error bar corresponds to the precision of the measurements

the origin, whereas *Figure 3* shows that the 'bond' effect gives rise to an effective additional thickness δL on the sample, thus increasing t_c and decreasing α from their true values. It should be noted that these lines are deliberately drawn through the two data points for the thicker samples since for the thinnest sample (1.5 mm) τ_1 becomes so short (1.2–2.2 sec) that we expect a much larger error from other sources. δL is seen to be about 0.1–0.2 mm and would cause 5–10% decrease in α for a sample 4 mm in thickness. These figures are probably indicative of the accuracy which could be expected from our data. If necessary, one could of course carry out measurements on samples of several thickness such as we have done for PC, and deduce α from the slopes of the $(t_c)^{1/2}$ vs. L graphs instead. Even though this is rather tedious it should thus be possible to eliminate the bond effect and obtain much more accurate results. However, in the other measurements, the thickness for each sample is chosen such that the accuracy estimated from the above criterion is better than 10%. The required thickness varies from 3 to 6 mm and the associated τ_1 are about 4 to 15 sec.

Sample

The samples of PC (Lexan) and POM (Delrin) were machined from commercially available rods. The PVF_2 sample was machined from a 3.5 mm thick sheet which were prepared by pressing powder (obtained from Cellomer Associates Inc.) at 180°C and then cooling slowly to room temperature. The PET sample was prepared from 0.7 mm thick sheets kindly supplied by ICI Ltd. About 18 sheets of width 3.5 mm and varying length were glued together (Araldite being used as the cementing agent) to form an approximate disc of diameter 1.3 mm, the two surfaces of which were then polished flat. In this configuration the sheets and epoxy are parallel to the direction of heat flow. Since the thermal diffusivity of PET and the epoxy are comparable there is no need to correct for the effect of the small amount of epoxy (~3%) present.

The densities of all the samples were determined by flotation method and the volume fraction crystallinities X were calculated from the known densities of the amorphous and crystalline phases. The crystallinities obtained for PC, PET, PVF_2 and POM are 0, 0, 0.53 and 0.70, respectively.

RESULTS AND DISCUSSION

Thermal diffusivity

We first discuss the results for PC (*Figure 4*) and compare them with Steere's thermal diffusivity measurements[8] (curve B, *Figure 4*), obtained by observing temperature change at a fixed distance from a thin foil heater; and also with Eiermann's[9] thermal conductivity (K) data (curve A) obtained by the steady heat-flow method, which we convert to α through the relation $\alpha = K/\rho C$, using literature[10,11] values for the specific heat C. The accuracy of the C measurements is usually better than 1%, so the error of ±5% in the curve A arises mainly from the K data. The accuracy of Steere's measurements was quoted at 2%[12] but the large discrepancy (25%) between B and A casts some doubt on this claim. Falling midway between B and A, our data can be considered to be in reasonable agreement with either set, since realistically the combined error between any two sets probably exceeds 15%.

Figure 5 illustrates the thermal diffusivity α as functions

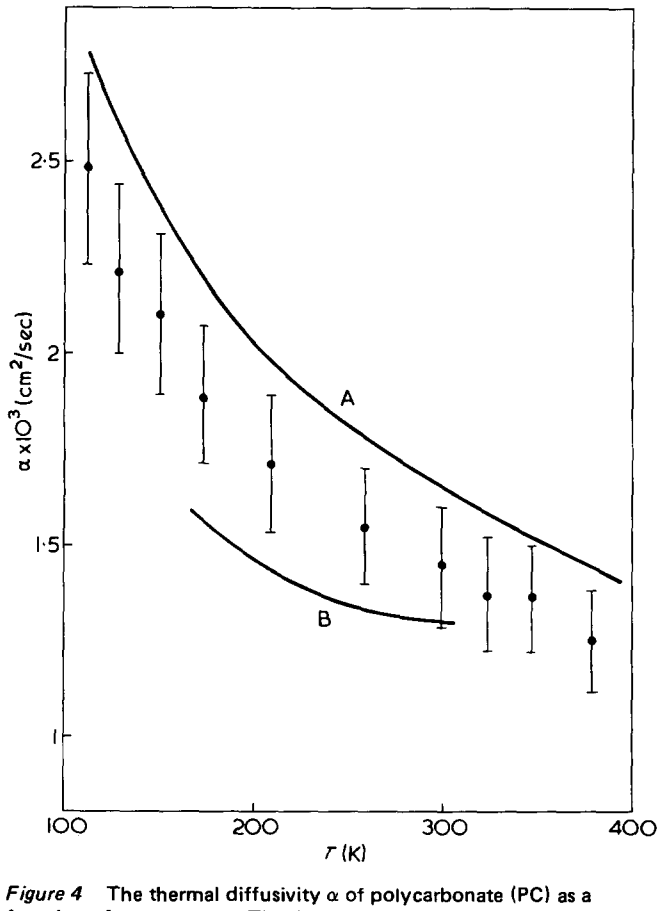

Figure 4 The thermal diffusivity α of polycarbonate (PC) as a function of temperature. The data are obtained for the sample of thickness 3.84 mm without correcting for the 'bond effect'. The ±10% error bar denotes the accuracy of the measurement. A, Eiermann's data (ref 9); B, Steere's data (ref 8)

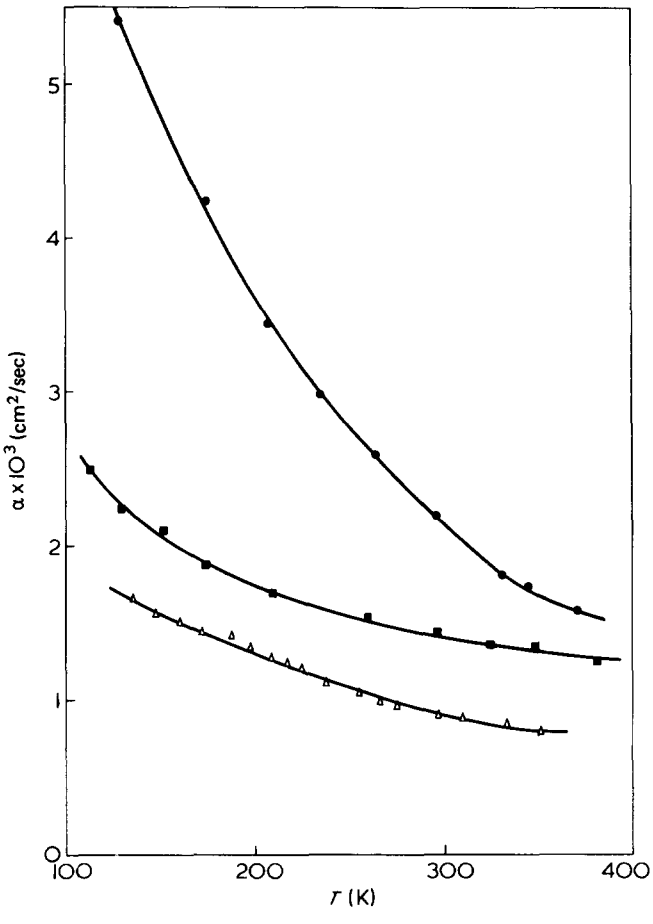

Figure 5 The thermal diffusivity α of PC (■), PVF_2 (△) and POM (●) as functions of temperature

of temperature of PC, PVF_2 and POM, which have widely different crystallinities, yet they all show similar temperature dependence: it decreases with increasing temperature, even though the decrease is much faster for the highly crystalline POM ($X = 0.7$). A somewhat surprising feature is that α of the amorphous PC is about 50% higher than that of PVF_2, which has a crystallinity ot 0.53, implying that the thermal diffusivity of the crystallites in PVF_2 is not much higher than that of the amorphous phase.

Thermal conductivity of PC, PVF_2 and POM

Next we consider the thermal conductivity (computed from α and the literature values of C[10,11,13,14]) shown in *Figure 6*. To have some theoretical understanding of its behaviour, let us first briefly discuss the structure of a semicrystalline polymer. A bulk crystallized sample of this material has a spherulitic structure composed of lamellar crystals and the interlamellar amorphous regions. The lamellae in turn are composed of mosaic crystalline blocks of size 100–300Å, with boundaries defined by dislocations[15–18]. While Takayanagi and Kajiyama[19] have termed the interlamellar amorphous regions and the intermosaic block regions as the amorphous state of the first and second kind, respectively, we will consider these two kinds of amorphous regions as identical as a first approximation, so a semicrystalline sample can be treated as a two-phase material with roughly cubic crystallites of size 100–300Å.

A number of models exist for the thermal conductivity of such a system, which is expected to depend on the conductivity K_a of the matrix (the amorphous regions in our case), the conductivity K_c of the dispersed phase (the crystallites) and the volume fraction X of the dispersed phase. Naturally the simplest possible arrangements for the two phases are the parallel and series arrangements, and we expect a real two-phase material to correspond to a combination of the two. In the latter case the K *versus* X curve would always lie between these two limiting curves. One such model is due to Maxwell[20], who showed that K for a system composed of spheres randomly distributed in a matrix is given by:

$$\frac{K}{K_a} = \frac{k + 2 - 2X(1-k)}{k + 2 + X(1-k)} \tag{1}$$

where $k = K_c/K_a$. Since the interaction among spheres is treated only in an average manner the model is strictly valid only for low X, say up to 0.3. By assuming that the spheres form a cubical array Rayleigh[21] and Meredith and Tobias[22] were able to take into account the effect of a number of nearby neighbour spheres and thus obtain an expression valid to $X = 0.5$. The results of Maxwell and Meredith and Tobias are very close to each other at low X but the difference increases with X, reaching about 20% at $X = 0.5$. Considering the primitive state of our knowledge of K of polymers it seems justified to use Maxwell model up to $X = 0.5$ but for even higher X its application should be regarded as simply empirical. As a matter of fact, Eiermann[23] employed Maxwell's model in the analysis of K of a number of polymers with crystallinity up to 0.88, from which K_a and K_c were deduced.

Another simple model[24,25] which is also applicable for a

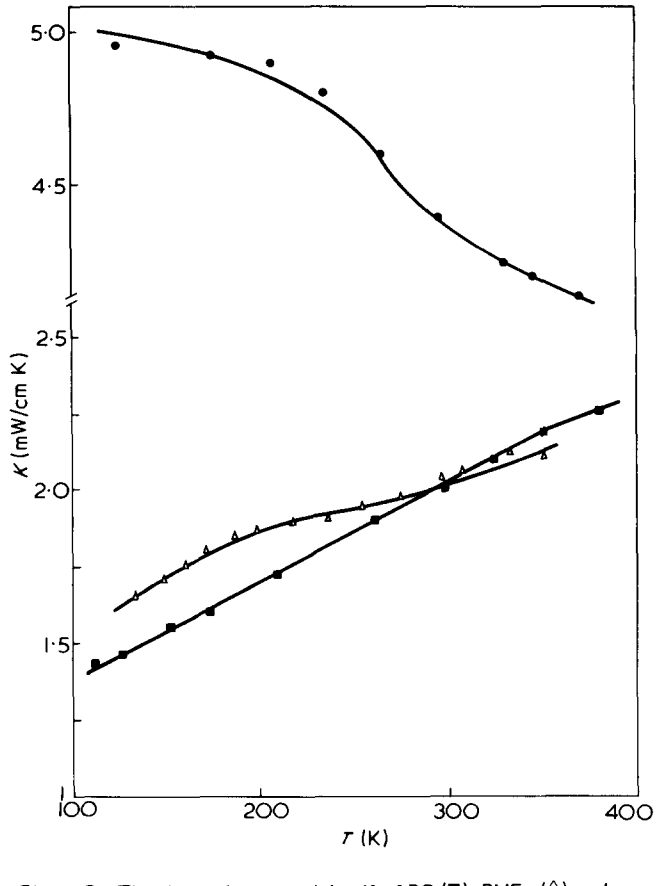

Figure 6 The thermal conductivity K of PC (■), PVF_2 (△) and POM (●) as functions of temperature.

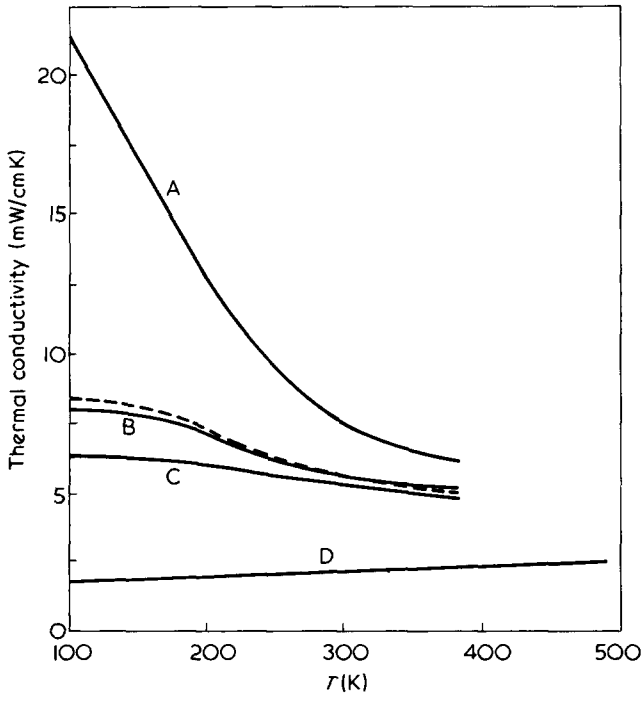

Figure 7 The thermal conductivity K_c of the crystallites of POM deduced from different models: A, series model; B, Maxwell's model (equation 1); C, parallel model; D, K_a, thermal conductivity of the amorphous matrix obtained by extrapolating the data for the melt. – – –, Series–parallel model (equation 2)

wide temperature range assumes that an amorphous fraction f is in parallel with the remaining $1-f$ of the material which is composed of a series arrangement of amorphous and crystalline regions. Although the dominant resistive mechanism at low temperature is due to boundary resistance at amorphous–crystalline interfaces, this effect becomes unimportant above 100K and the thermal conductivity is then given by:

$$K = \frac{(1-f)^2}{X/K_c + (1-f-X)/K_a} + fK_a \qquad (2)$$

Equation (2) will of course reduce to the series and parallel model, respectively, if f is set at 0 or $1-X$. It has been shown[24,25] that equation (2) works quite well for polymers if f is set at 0.1 for samples with crystallinity between 0.3 and 0.9.

Let us now look at our POM data in light of the above four models. Since it is impossible to prepare bulk solid samples of either completely amorphous or crystalline POM we can only attempt to obtain estimates of K_c from our analysis, assuming that K_a can be obtained by extrapolating the data for the melt[15,26], and a linear temperature dependence with a 40% decrease between 490 and 100K, a trend generally obeyed by amorphous polymers. From this estimated K_a and the measured values of K at $X = 0.7$ K_c has been calculated according to the various models and plotted in *Figure 7*. It is clear that the magnitude of K_c is rather model-dependent, varying by a factor of 4 at low temperature. However, an expected general trend also seems clear: K_c increases with decreasing temperature, which is characteristic of crystalline solids, since the thermal resistance arising from both phonon–phonon Umklapp process and phonon–defect scattering becomes less important at low temperature.

We note that the K_c obtained here is only a measure of the average thermal conductivity of a crystallite: it has been theoretically and experimentally[25,27,28] shown that the conductivity along the chains ($K_{c//}$) of a crystallite is very much larger than that across the chains ($K_{c\perp}$). For polyethylene, a polymer with C–C bonding along chains, $K_{c//} \simeq 320$ mW/cmK at 100K while $K_{c\perp} \simeq 6$ mW/cmK and $K_a \simeq 1.8$ mW/cmK[28]. The relatively low K_c of 8 mW/cmK obtained for POM, which is a polymer with C–O bonds along chains, probably reflects the contribution of the more resistive component across the chains.

Using Maxwell's model we have also generated a series of theoretical curves for POM at various values of X (*Figure 8*). While at low $X(\leqslant 0.3)$ K follows the temperature dependence of K_a and increases slowly with temperature, at high $X(X \geqslant 0.7)$ it has the same trend as K_c. At $X = 0.5$, K is very sensitive to the relative magnitude and temperature dependence of K_a and K_c and in this case it first increases and then decreases with temperature. With these theoretical curves as a guide we see that the very low

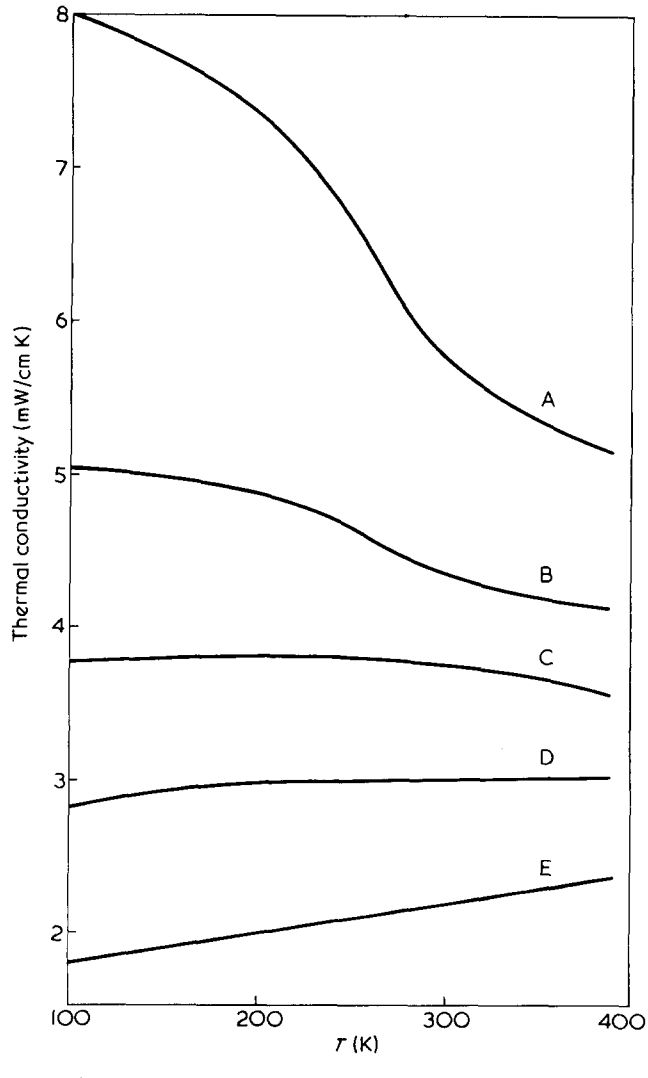

Figure 8 Theoretical thermal conductivity of POM for different degrees of crystallinity calculated from Maxwell's model. K_c and K_a are, respectively, the thermal conductivities of the crystalline and amorphous regions. A, K_c; B, $X = 0.7$; C, $X = 0.5$; D, $X = 0.3$; E, K_a

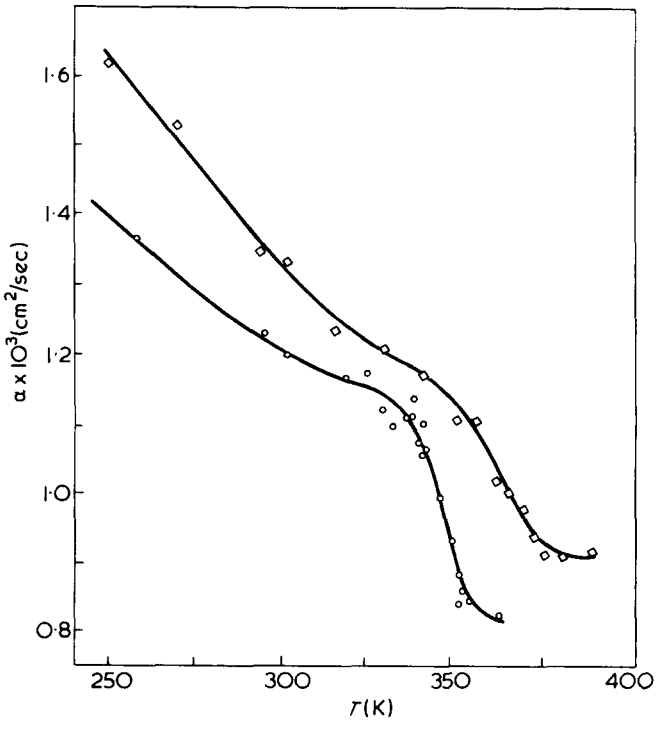

Figure 9 The thermal diffusivity α of PET as functions of temperature: ○, amorphous; ◇, annealed 4 h at 120°C ($X \simeq 0.3$)

K values for PVF_2 (almost the same as amorphous polymers) arises from having a K_c much lower than that of POM.

Glass transition of PET

If amorphous PET (which has a dilatometric glass transition temperature at 340K) is annealed crystallization does not occur until 363°C, and above this temperature PET first exhibits a 'stepwise' crystallization and then a slow secondary crystallization. It is therefore a very suitable material for the study of the behaviour of α near the glass transition and the effect of crystallization.

Figure 9 shows the results of these studies. It is clearly seen that there is an abrupt drop in α of about 30% between 340 and 355K while above and below this range the change of α is much more gradual. Crystallization at 393K (120°C) for 4 h results in a crystallinity of about 0.3 and an α which is about 10% higher at temperatures below the glass transition. For this semicrystalline sample the drop in α is slightly less, the transition region is more diffused (350–380K) and the midpoint T_d of this region is about 17K higher. It is interesting to note that mechanical modulus data also show similar trends[29,30] and these have been attributed to the fact that the crystallites now impose considerable constraints on the amorphous regions thus impeding molecular motion especially near the glass transition.

The thermal conductivity of amorphous PET (computed from our data and the literature values[31] of C) is illustrated in *Figure 10*. The 10% jump in K near 340K may be an artifact caused by the difference in the transition point as revealed by the α ($T_d \sim 348$K) and C($T_d \sim 340$K) data, which in turn reflects the different time scale (about 10 sec and 1000 sec for α and C measurements, respectively) involved. However, the large change in slope near T_d has previously been observed[9,32] in other amorphous

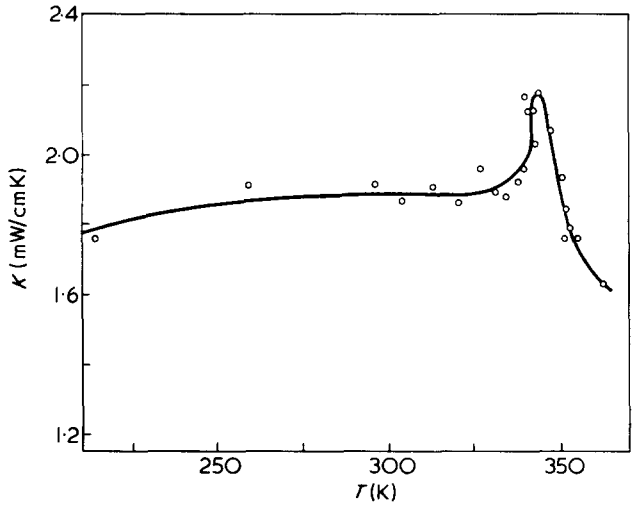

Figure 10 The thermal conductivity K of amorphous PET as a function of temperature

polymers by workers employing the steady heat-flow method.

In conclusion, it seems that the flash method is quite suitable for the study of the thermal diffusivity of polymers. Since it is not necessary to apply large pressure between the sample and the heater or heat sink in order to attain good thermal contact, the technique is especially valuable for investigating polymers in the rubbery state where the results may be severely affected by sample deformation. The possibility of using comparatively small sample is a further advantage in work on oriented polymers, for which the preparation of large samples is rather difficult.

REFERENCES

1 Parker, W. J., Jenkins, R. J., Butler, C. P. and Abbott, G. L. *J. Appl. Phys.* 1961, **32**, 1679
2 Deem, H. W. and Wood, W. D. *Rev. Sci. Instrum.* 1962, **33**, 1107
3 Taylor, R. *Br. J. Appl. Phys.* 1965, **16**, 508
4 Shaw, D. and Goldsmith, L. A. *J. Sci. Instrum.* 1966, **43**, 594
5 Simpson, A. and Stuckes, A. D. *J. Phys. (C)* 1971, **4**, 1710
6 Righini, F. and Cezairliyan, A. *High Temp. High Pressures* 1973, **5**, 481
7 Cape, J. A. and Lehman, G. W. *J. Appl. Phys.* 1963, **34**, 1909
8 Steere, R. C. *J. Appl. Polym. Sci.* 1966, **10**, 1673
9 Eiermann, K. *Kunstoffe* 1965, **55**, 335
10 Dainton, F. S., Evans, D. M., Hoare, F. E. and Melia, T. P. *Polymer* 1962, **3**, 263
11 O'Reilly, J. M., Karasz, F. E. and Bair, H. E. *J. Polym. Sci. (C)* 1963, **6**, 109
12 Steere, R. C. *J. Appl. Phys.* 1966, **37**, 335
13 Hellwege, K. H., Knappe, W. and Wetzel, W. *Kolloid Z* 1962, **180**, 126
14 Lee, W. K. and Choy, C. L. *J. Polym. Sci.* 1975, **13**, 619
15 Statton, W. D. *J. Polym. Sci. (C)* 1967, **18**, 33
16 Hosemann, R. *J. Polym. Sci. (C)* 1967, **20**, 1
17 Kavesh, S. and Schultz, J. M. *J. Polym. Sci. (A-2)* 1970, **8**, 243
18 Loboda-Cackovic, J., Hosemann, R., Cackovic, H., Ferrero, F. and Ferracini, E. *Polymer* 1976, **17**, 303
19 Takayanagi, M. and Kajiyama, T. *J. Macrom. Sci. (B)* 1973, **8**, 1
20 Maxwell, J. C. 'A Treatise on Electricity and Magnetism', Clarendon Press, Oxford, 1892, Vol 1, pp 435
21 Rayleigh, Lord *Phil. Mag.* 1892, **34**, 481
22 Meredith, R. E. and Tobias, C. W. *J. Appl. Phys.* 1960, **31**, 1270
23 Eiermann, K. *Kolloid Z.* 1965, **201**, 3

24 Choy, C. L. and Greig, D. *J. Phys. (C)* 1975, **8**, 3121
25 Choy, C. L. *Polymer* to be published
26 Shoulberg, R. B. *J. Appl. Polym. Sci.* 1963, **7**, 1597
27 Burgess, S. and Greig, D. *J. Phys. (C)* 1975, **8**, 1637
28 Gibson, A. G., Greig, D., Sahota, M., Ward, I. M. and Choy, C. L. *J. Polym. Sci. (Polym. Lett. Edn)* to be published
29 Illers, K. H. and Breuer, H. *J. Colloid. Sci.* 1963, **18**, 1
30 Takayanagi, M. *High Polym.* 1961, **10**, 289
31 Smith, C. W. and Dole, M. *J. Polym. Sci.* 1956, **20**, 37
32 Eiermann, K. and Hellwege, K. H. *J. Polym. Sci.* 1962, **57**, 99